

Vibrational Fine Structure of the Ligand Field Absorption Band of Halogenoammine Cobalt(III) Complexes

Kunimasa FUKUDA and Akio URUSHIYAMA*

Department of Chemistry, Faculty of Science, Rikkyo University, Nishiikebukuro, Toshima-ku, Tokyo 171

(Received December 13, 1977)

The crystal absorption spectra of some halogenoammine complexes of Co(III) were measured at liquid helium temperature. The vibrational fine structures observed for the spin-allowed ligand field bands were interpreted in terms of a vibronic intensity mechanism in comparison with the vibrational frequencies of the skeletons. It was found that all the vibrational fine structures consist of the unquantal progression of totally symmetric Co-N stretching vibration. This suggests that the equilibrium Co-N distances of these complexes are elongated in the ligand field electronic excited state as compared with those in the ground state.

The vibrational fine structure of the ligand field absorption band of $[\text{Co}(\text{NH}_3)_6]^{3+}$ was studied by Wentworth.¹⁾ He found in his low temperature optical study that the vibrational fine structure of the ${}^1\text{T}_{1g} \leftarrow {}^1\text{A}_{1g}$ band of the complex consists of the unquantal progression correlated to the totally symmetric Co-N stretching vibration of the CoN_6 skeleton. Since then some reports concerning $[\text{Co}(\text{en})_3]^{3+}$ have appeared.^{2,3)} A study was carried out for the mixed ligand complexes.⁴⁾ In the present study, the crystal absorption spectra of some halogenoammine complexes of Co(III) have been measured at liquid helium temperature, the vibrational fine structure of the ligand field bands of the complexes in reduced symmetries being of much interest. Complex fine structure could be observed for almost all the bands in the visible region. The observed fine structures were interpreted on the basis of the infrared and Raman data of the complexes assuming a vibronic intensity scheme.

Experimental

All the complex salts were prepared according to the procedures reported previously⁵⁾ except for *trans*- $[\text{CoCl}_2(\text{NH}_3)_4]_3\text{[Co(CN)}_6\text{]}$ and *trans*- $[\text{CoBr}_2(\text{NH}_3)_4]_3\text{[Co(CN)}_6\text{]}$. Excellent single-crystals of $[\text{CoF}(\text{NH}_3)_5]\text{Cl}_2 \cdot 2\text{H}_2\text{O}$ for the transmission spectroscopy could be obtained by evaporation of the aqueous solution in a vacuum desiccator. In the cases of $[\text{Co}(\text{NH}_3)_6]\text{[Co(CN)}_6\text{]}$, $[\text{CoCl}(\text{NH}_3)_5]\text{Cl}_2$, and $[\text{CoBr}(\text{NH}_3)_5]\text{Br}_2$, excellent crystals could be obtained when the aqueous solutions of $\text{K}_3\text{[Co(CN)}_6\text{]}$, 1M HCl, and 1M HBr, respectively, were dispersed extremely slowly into each of the solutions containing the corresponding complex cation. The fine crystalline pow-

ders of *trans*- $[\text{CoCl}_2(\text{NH}_3)_4]_3\text{[Co(CN)}_6\text{]}$ and *trans*- $[\text{CoBr}_2(\text{NH}_3)_4]_3\text{[Co(CN)}_6\text{]}$ were precipitated immediately from the freshly prepared aqueous solutions of *trans*- $[\text{CoCl}_2(\text{NH}_3)_4]\text{Cl}$ and *trans*- $[\text{CoBr}_2(\text{NH}_3)_4]\text{ClO}_4$, respectively, by adding an aqueous solution of $\text{K}_3\text{[Co(CN)}_6\text{]}$ at 0 °C. The diffuse reflectance spectra in the visible region and the infrared absorption spectra of the crystals suggest that the skeletons of the complexes are retained throughout these procedures. Found: Co, 29.1%. Calcd for *trans*- $[\text{CoCl}_2(\text{NH}_3)_4]_3\text{[Co(CN)}_6\text{]}$: Co, 29.1%. Found: Co, 22.0%. Calcd for *trans*- $[\text{CoBr}_2(\text{NH}_3)_4]_3\text{[Co(CN)}_6\text{]}$: Co, 21.9%.

The visible absorption spectra of the crystalline samples were measured with an apparatus (Fig. 1) consisting of a JASCO model CT-50 monochromater, a specially designed liquid helium optical cryostat, and a HTV model C767 photon counting system. The liquid helium flowed from the container of the cryostat to a specially designed cooling stage made of a copper block through a tunnel bored inside it. Single-crystals of appropriate size ($\sim 0.2 \times \sim 0.2 \times \sim 0.02$ mm) were mounted over a pinhole ($\phi = 0.15$ mm) in an indium plate, which was then placed on the cooling stage of the cryostat. The sample crystals were made large enough to cover the pinhole completely for the measurements. Silicone grease ensured good thermal contact between the crystal, indium plate, and cooling stage. Silicone grease mulls of the powdered sample were mounted on a small glass plate, and placed on the cooling stage in a similar way to that for the single-crystal measurements. A thermocouple (gold-iron: chromel) indicated the cooling of samples to liquid helium temperature throughout the measurements. The values of transmission light recorded were corrected by those of the blank measurement adjusting the transmittance to unity in the lower wavenumber region where the samples could not absorb.

Results and Discussion

$[\text{Co}(\text{NH}_3)_6]^{3+}$. The single crystal absorption spectrum of $[\text{Co}(\text{NH}_3)_6]\text{[Co(CN)}_6\text{]}$ is shown in Fig. 2. Clear vibrational structure is superimposed on the ${}^1\text{T}_{1g} \leftarrow {}^1\text{A}_{1g}$ band of $[\text{Co}(\text{NH}_3)_6]^{3+}$ as reported by Wentworth.¹⁾ However, no structure could be detected on the ${}^1\text{T}_{2g} \leftarrow {}^1\text{A}_{1g}$ band in the near-ultraviolet region. The crystal is hexagonal with the space group $\text{R}\bar{3}$ and the precise symmetry of $[\text{Co}(\text{NH}_3)_6]^{3+}$ is S_6 .⁷⁾ However, the polarized absorption spectra with the light parallel and perpendicular to the crystal *c* axis appear to be almost identical.

Most of the lines can be explained in terms of the unquantal progression of the $\nu_1(\text{a}_{1g})$ Co-N stretching vibration of the combination, $\nu_1 + (N+n)\nu_1(\text{a}_{1g})$,

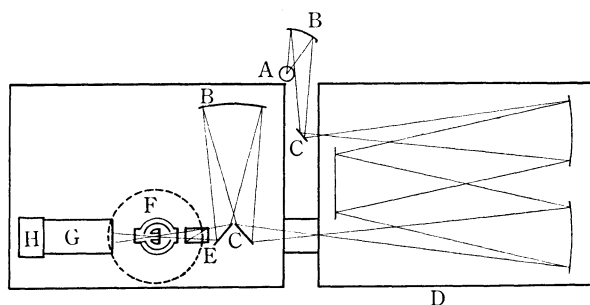


Fig. 1. Apparatus for low temperature optical study. A: Tungsten lamp, B: mirror, C: mirror, D: monochromater (CT-50), E: polarizer, F: cryostat, G: photomultiplier (HTV R649S or R585S), H: pre. amp.

TABLE 1. SKELETAL VIBRATIONAL FREQUENCIES OF Co(III) COMPLEXES^{a)}

Compound	Vibrational frequency, cm ⁻¹					
O _h symmetry	$\nu_1(a_{1g})$	$\nu_3(t_{1u})$	$\nu_4(t_{1u})$			
[Co(NH ₃) ₆] ³⁺	490 ^{b)}	480 ^{b)}	331 ^{b)}			
D _{4h} symmetry	$\nu_1(a_{1g})$	$\nu_2(a_{1g})$	$\nu_9(e_u)$	$\nu_{10}(e_u)$	$\nu_{11}(e_u)$	
<i>trans</i> -[CoCl ₂ (NH ₃) ₄] ⁺	275 ^{b)}	492 ^{b)}	501 ^{c)}	178 ^{c)}	290 ^{c)}	
<i>trans</i> -[CoBr ₂ (NH ₃) ₄] ⁺		482 ^{d)}	486 ^{c)}	140 ^{c)}	295 ^{c)}	
C _{4v} symmetry	$\nu_1(a_1)$	$\nu_3(a_1)$	$\nu_8(e)$	$\nu_9(e)$	$\nu_{10}(e)$	$\nu_{11}(e)$
[CoF(NH ₃) ₅] ²⁺		494 ^{d)}	504 ^{c)}	309 ^{c)}	249 ^{c)}	328 ^{c)}
[CoCl(NH ₃) ₅] ²⁺	274 ^{b)}	485 ^{b)}	487 ^{c)}	285 ^{c)}	200 ^{c)}	325 ^{c)}
[CoBr(NH ₃) ₅] ²⁺		483 ^{d)}	501 ^{c)}			319 ^{c)}

a) Normal modes are denoted according to Ref. 6a. b) Frequencies reported in Ref. 6a. c) Frequencies reported in Ref. 6b. d) Present work for the perchlorates.

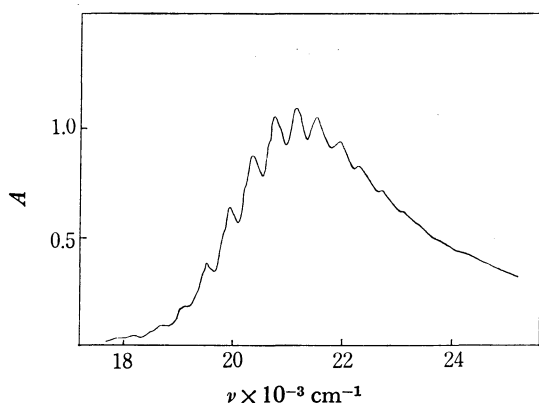


Fig. 2. Crystal absorption spectrum of [Co(NH₃)₆]-[Co(CN)₆] at 4.2 K (with polarized light parallel to the crystal c axis).

where ν_1 =ungerade vibration, N =integer, and $n=0, 1, 2, \dots$, assuming a vibronic intensity scheme. The vibrational frequencies of the ammine complexes of Co(III) have been studied by several workers.⁶⁾ The frequencies referred to in the present study are given in Table 1. The average spacing of 402 cm⁻¹ seems to be reasonable for the $\nu_1(a_{1g})$ vibrational frequency at the ${}^1T_{1g}$ electronic excited state. It represents an 18% reduction in the $\nu_1(a_{1g})$ vibrational frequency as compared with the ground state value of 490 cm⁻¹. The electronic excitation into the antibonding e_g orbital may elongate the Co-N bond distances to some extent, giving rise to this frequency reduction. Each line could be resolved into two or more components. However, measurement with higher resolution is necessary for further discussion of the structure.

trans-[CoCl₂(NH₃)₄]⁺ and *trans*-[CoBr₂(NH₃)₄]⁺. The low temperature mull spectra of *trans*-[CoCl₂(NH₃)₄]₃[Co(CN)₆] and *trans*-[CoBr₂(NH₃)₄]₃[Co(CN)₆] are shown in Figs. 3 and 4, respectively. The bands in the 16000—18500 cm⁻¹ region are assigned to the ${}^1E_g[{}^1T_{1g}(O_h)] \leftarrow {}^1A_{1g}$ transition and those in the 18500—22000 cm⁻¹ region to the ${}^1A_{2g}[{}^1T_{1g}(O_h)] \leftarrow {}^1A_{1g}$ transition in D_{4h} symmetry. Some indistinct structure was found on the ${}^1E_g \leftarrow {}^1A_{1g}$ band of *trans*-[CoCl₂(NH₃)₄]⁺, whereas no structure could be detected for the band of *trans*-[CoBr₂(NH₃)₄]⁺. Due to its

TABLE 2. SELECTION RULE FOR THE LIGAND FIELD ABSORPTION BAND OF Co(III) COMPLEXES IN REDUCED SYMMETRY

Transition	Electronic	Vibronic
D _{4h}		Vibrational species
${}^1E_g \leftarrow {}^1A_{1g}$	forbidden	$\begin{cases} \text{allowed}(xy) \\ \text{allowed}(xy) \\ \text{allowed}(xyz) \end{cases}$ a_{2u} b_{2u} e_u
${}^1A_{2g} \leftarrow {}^1A_{1g}$	forbidden	allowed(xy) e_u
C _{4v}		
${}^1E \leftarrow {}^1A_1$	allowed(xy)	$\begin{cases} \text{allowed}(xy) \\ \text{allowed}(xy) \\ \text{allowed}(z) \end{cases}$ b_1 b_2 e
${}^1A_2 \leftarrow {}^1A_1$	forbidden	allowed(xy) e

TABLE 3. OBSERVED OPTICAL TRANSITIONS AND ASSIGNMENTS FOR THE ${}^1A_{2g} \leftarrow {}^1A_{1g}$ TRANSITION OF *trans*-[CoCl₂(NH₃)₄]⁺ AT 4.2 K

Peak	Energy, cm ⁻¹	Assignment
1c	18450	${}^1A_{2g} + \nu_9 + (N+1)\nu_2$
2c	18880	$+ \nu_9 + (N+2)\nu_2$
3a	19040	$+ \nu_{10} + (N+3)\nu_2$
3b	19150	$+ \nu_{11} + (N+3)\nu_2$
3c	19290	$+ \nu_9 + (N+3)\nu_2$
4b	19580	$+ \nu_{11} + (N+4)\nu_2$
4c	19720	$+ \nu_9 + (N+4)\nu_2$
5b	19990	$+ \nu_{11} + (N+5)\nu_2$
5c	20130	$+ \nu_9 + (N+5)\nu_2$
6b	20400	$+ \nu_{11} + (N+6)\nu_2$
6c	20560	$+ \nu_9 + (N+6)\nu_2$
7b	20810	$+ \nu_{11} + (N+7)\nu_2$
7c	20980	$+ \nu_9 + (N+7)\nu_2$
8b	21150	$+ \nu_{11} + (N+8)\nu_2$
8c	21300	$+ \nu_9 + (N+8)\nu_2$

low resolution, no assignment of the structure is possible in the present study.

In the ${}^1A_{2g} \leftarrow {}^1A_{1g}$ band region, predominant progressions were found with average spacings of 422 and 411 cm⁻¹, for *trans*-[CoCl₂(NH₃)₄]⁺ and *trans*-[CoBr₂(NH₃)₄]⁺, respectively. These frequencies can naturally be correlated to the $\nu_2(a_{1g})$ Co-N stretch-

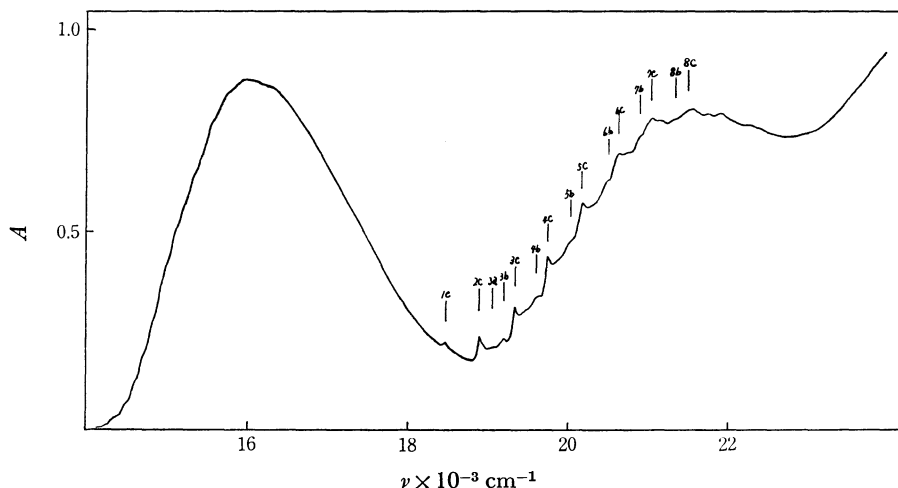


Fig. 3. Crystal absorption spectrum of *trans*-[CoCl₂(NH₃)₄]₃[Co(CN)₆] at 4.2 K (mull method).

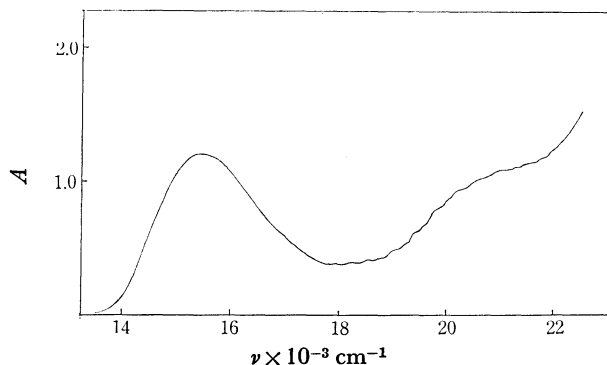


Fig. 4. Crystal absorption spectrum of *trans*-[CoBr₂(NH₃)₄]₃[Co(CN)₆] at 4.2 K (mull method).

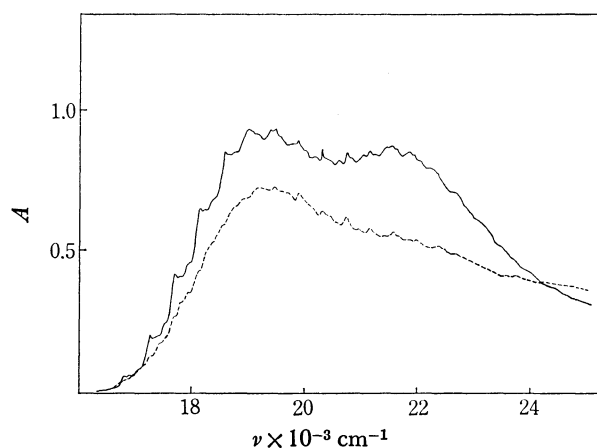


Fig. 5. Polarized absorption spectra of [CoF(NH₃)₅]-Cl₂·2H₂O at 4.2 K.

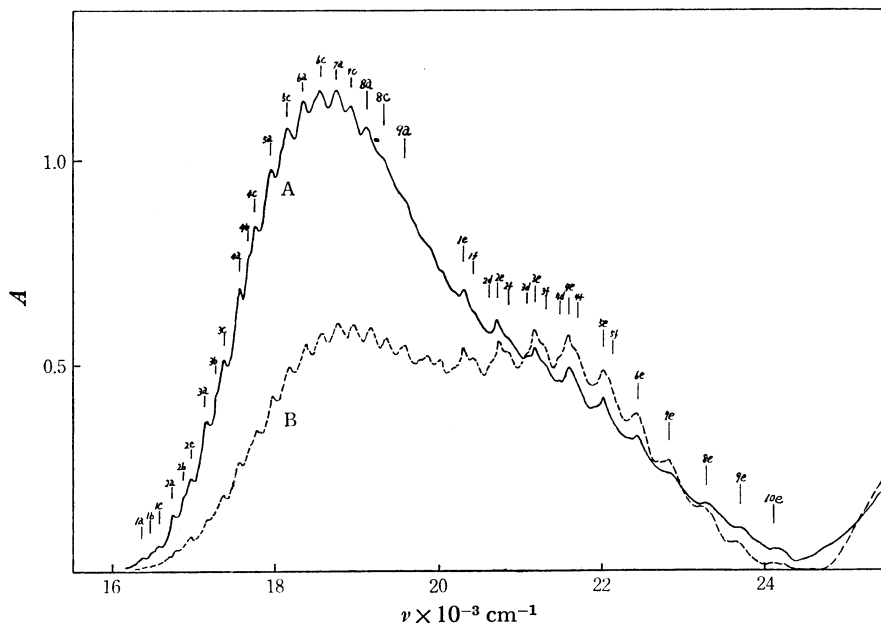
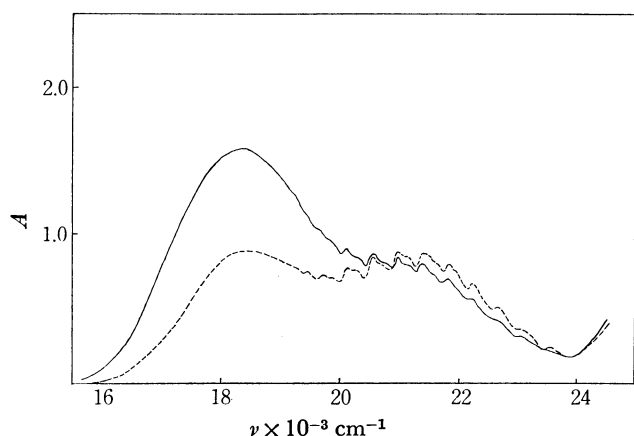
ing vibration of the *trans*-CoX₂N₄ groups in the electronic excited state. The frequency reduction of the ν_2 vibration were estimated to be 14 and 15% for *trans*-[CoCl₂(NH₃)₄]⁺ and *trans*-[CoBr₂(NH₃)₄]⁺, respectively, as compared with the values in the ground state. These findings suggest that the complexes are displaced along the Q₂ normal coordinate in the ¹A_{2g} electronic excited state. The coordinate has been analysed to consist mainly of the symmetric Co-N bond length changes in these complexes.⁶ The ¹A_{2g} ← ¹A_{1g} transition corresponds to an electronic excitation from the d_{xy} orbital to the antibonding d_{x²-y²} orbital. It can be surmised that the Co-N equilibrium distances are elongated to some extent in the ¹A_{2g} electronic excited state as compared with those in the ground state. This is in line with the present results.

The selection rules of the ligand field absorption bands are given in Table 2. For the ¹A_{2g} ← ¹A_{1g} transition, only the e_u vibrational mode can couple with the electronic state to give a vibronically allowed transition. Thus, the vibronic patterns observed should be characterized by the ν_9 (e_u): Co-N str., ν_{10} (e_u): Co-X bend., and ν_{11} (e_u): N-Co-N def. vibrations combined with the totally symmetric vibration. If we compare the energy differences between adjacent peaks with the infrared absorption energies, the assignments (Table 3) seem reasonable, although the

excited state vibrational frequencies may somewhat differ from those in the ground state. The vibronic pattern of the ¹A_{2g} ← ¹A_{1g} band of *trans*-[CoBr₂(NH₃)₄]⁺ can be interpreted similarly, although the components of ν_{11} (e_u) were indistinct.

[CoF(NH₃)₅]²⁺, [CoCl(NH₃)₅]²⁺, and [CoBr(NH₃)₅]²⁺. The polarized absorption spectra of [CoF(NH₃)₅]-Cl₂·2H₂O, [CoCl(NH₃)₅]-Cl₂, and [CoBr(NH₃)₅]-Br₂ are shown in Figs. 5, 6, and 7, respectively. They were measured by polarized light along the extinction directions perpendicular to the crystal face which exhibited the most distinct dichroism under a polarizing microscope. A distinct splitting of the ¹T_{1g}(O_h) ← ¹A_{1g}(O_h) band was observed in each case. The bands at lower energy are assigned to the ¹E[¹T_{1g}(O_h)] ← ¹A₁ transition and the higher energy ones to the ¹A₂[¹T_{1g}(O_h)] ← ¹A₁ transition in C_{4v} symmetry. A good deal of vibrational structure was observed for almost all the bands.

In the ¹E ← ¹A₁ band region of [CoCl(NH₃)₅]²⁺, distinct lines appeared apparently with progression spacing of 200 cm⁻¹, weak components being found in the alternate gaps between these lines. However, by careful inspection of the relative intensities of the peaks,

Fig. 6. Polarized absorption spectra of $[\text{CoCl}(\text{NH}_3)_5]\text{Cl}_2$ at 4.2 K.Fig. 7. Polarized absorption spectra of $[\text{CoBr}(\text{NH}_3)_5]\text{Br}_2$ at 4.2 K.

the vibronic pattern could be characterized to consist of the progression with average spacing of 397 cm^{-1} in three components. This frequency can be correlated to the $\nu_3(a_1)$: Co-N str. vibration in the ${}^1\text{E}$ electronic excited state, representing a 20% frequency reduction in comparison with the ground state value of 495 cm^{-1} . Stanko⁴⁾ studied the polarized absorption spectra of $[\text{CoX}(\text{NH}_3)_5]\text{SiF}_6$, where $\text{X}=\text{Cl}, \text{Br}, \text{CN}$, and concluded that the main features of the ligand field absorption bands of these complexes can be accounted for by a vibronic intensity mechanism. He also showed on the basis of intensity calculation that the $\nu_8(e)$: Co-N str., $\nu_{10}(e)$: Co-X bend., and $\nu_{11}(e)$: N-Co-N def. vibrational modes play an important role in the vibronic mechanism of the ${}^1\text{E}$ band of $[\text{CoCl}(\text{NH}_3)_5]^{2+}$. It was found in the present study that the A polarized spectrum (Fig. 6), which is thought to be rich with the xy-polarized spectrum of the complex because of the dominant emergence of the ${}^1\text{A}_2$ band, shows no vibrational component more than those observed in the B spectrum, which must be rich with

the z-polarized spectrum of the complex (Table 2). The best fit to experimental data when the energy differences between adjacent peaks are compared with the infrared frequencies of the e vibrational modes is shown in Table 4.

In the spectra of $[\text{CoF}(\text{NH}_3)_5]^{2+}$, the vibrational structure of the ${}^1\text{E}$ band appears in a different pattern for each polarization direction. This suggests that the a_2 and/or b_2 vibrational species responsible for the vibronic intensity along the xy axis of the complex are important for this band. However, the spacings of the progression were estimated to be 420 cm^{-1} . The frequency corresponds to the $\nu_3(a_1)$ vibration.

All the complexes in the present study show a complex fine structure in their ${}^1\text{A}_2 \leftarrow {}^1\text{A}_1$ band region.⁴⁾ Several components were found to form a progression for each complex. The intervals of the progression found in the spectra of $[\text{CoF}(\text{NH}_3)_5]\text{Cl}_2 \cdot 2\text{H}_2\text{O}$, $[\text{CoCl}(\text{NH}_3)_5]\text{Cl}_2$, and $[\text{CoBr}(\text{NH}_3)_5]\text{Br}_2$ were estimated to be 420, 419, and 429 cm^{-1} , respectively. These frequencies correspond to the $\nu_3(a_1)$ vibration in the ${}^1\text{A}_2$ excited state, representing frequency reductions of 15, 14, and 12%, respectively, as compared with the ground state values. The ${}^1\text{A}_2 \leftarrow {}^1\text{A}_1$ band of these complexes can be interpreted in terms of the vibronic intensity mechanism through the vibrations of e species (Table 2). The observed components can be assigned by considering the energy differences between adjacent peaks (Table 4). The vibronic patterns of the ${}^1\text{A}_2 \leftarrow {}^1\text{A}_1$ $[\text{CoF}(\text{NH}_3)_5]^{2+}$ and band of $[\text{CoBr}(\text{NH}_3)_5]^{2+}$ can be interpreted in a similar way to that for the chloro complex. The $\nu_{10}(e)$ components of $[\text{CoBr}(\text{NH}_3)_5]^{2+}$ are thought to be obscured due to the shift toward a position close to the $\nu_8(e)$ components because of the reduction in the $\nu_{10}(e)$ vibrational frequency of the complex.

The authors wish to express their thanks to Prof. Yukio Kondo, Rikkyo University, for his encouragement.

TABLE 4. OBSERVED OPTICAL TRANSITIONS AND ASSIGNMENTS IN THE 16000—24000 cm^{-1} REGION FOR $[\text{CoCl}(\text{NH}_3)_5]^{2+}$ AT 4.2 K

Peak	Energy, cm^{-1}	Assignment	Peak	Energy, cm^{-1}	Assignment
1a	16300	${}^1\text{E} + \nu_{10} + (N+1)\nu_3$	1e	20230	${}^1\text{A}_2 + \nu_{11} + (N+1)\nu_3$
1b	16400	$+ \nu_{11} + (N+1)\nu_3$	1f	20360	$+ \nu_8 + (N+1)\nu_3$
1c	16500	$+ \nu_8 + (N+1)\nu_3$	2d	20530	$+ \nu_{10} + (N+2)\nu_3$
2a	16700	$+ \nu_{10} + (N+2)\nu_3$	2e	20660	$+ \nu_{11} + (N+2)\nu_3$
2b	16820	$+ \nu_{11} + (N+2)\nu_3$	2f	20790	$+ \nu_8 + (N+2)\nu_3$
2c	16900	$+ \nu_8 + (N+2)\nu_3$	3d	20970	$+ \nu_{10} + (N+3)\nu_3$
3a	17100	$+ \nu_{10} + (N+3)\nu_3$	3e	21080	$+ \nu_{11} + (N+3)\nu_3$
3b	17220	$+ \nu_{11} + (N+3)\nu_3$	3f	21220	$+ \nu_8 + (N+3)\nu_3$
3c	17310	$+ \nu_8 + (N+3)\nu_3$	4d	21390	$+ \nu_{10} + (N+4)\nu_3$
4a	17500	$+ \nu_{10} + (N+4)\nu_3$	4e	21480	$+ \nu_{11} + (N+4)\nu_3$
4b	17610	$+ \nu_{11} + (N+4)\nu_3$	4f	21600	$+ \nu_8 + (N+4)\nu_3$
4c	17710	$+ \nu_8 + (N+4)\nu_3$	5e	21910	$+ \nu_{11} + (N+5)\nu_3$
5a	17890	$+ \nu_{10} + (N+5)\nu_3$	5f	22030	$+ \nu_8 + (N+5)\nu_3$
5c	18090	$+ \nu_8 + (N+5)\nu_3$	6e	22330	$+ \nu_{11} + (N+6)\nu_3$
6a	18290	$+ \nu_{10} + (N+6)\nu_3$	7e	22730	$+ \nu_{11} + (N+7)\nu_3$
6c	18480	$+ \nu_8 + (N+6)\nu_3$	8e	23180	$+ \nu_{11} + (N+8)\nu_3$
7a	18670	$+ \nu_{10} + (N+7)\nu_3$	9e	23600	$+ \nu_{11} + (N+9)\nu_3$
7c	18870	$+ \nu_8 + (N+7)\nu_3$	10e	24020	$+ \nu_{11} + (N+10)\nu_3$
8a	19070	$+ \nu_{10} + (N+8)\nu_3$			
8c	19280	$+ \nu_8 + (N+8)\nu_3$			
9a	19470	$+ \nu_{10} + (N+9)\nu_3$			

References

- 1) R. A. D. Wentworth, *Chem. Commun.*, **1965**, 532.
- 2) R. Dingle, *Chem. Commun.*, **1965**, 304.
- 3) R. G. Denning, *Chem. Commun.*, **1967**, 120.
- 4) J. A. Stanko, Ph. D. Thesis, University of Illinois, U. S. A. 1966. He studied single-crystals of $[\text{CoCl}(\text{NH}_3)_5]\text{SiF}_6$ and $[\text{CoBr}(\text{NH}_3)_5]\text{SiF}_6$ at liquid nitrogen temperature, and observed simple peaks with progressional spacings of

466 and 410 cm^{-1} , respectively, on the ${}^1\text{A}_2 \leftarrow {}^1\text{A}_1$ band.

5) "Gmelin Handbuch" **58**, Tl. B. 1964.

6) a) T. M. Loeher, J. Zinich, and T. V. Long II, *Chem. Phys. Lett.*, **7**, 183 (1970); b) L. Sacconi, A. Sabatini, and D. Gans, *Inorg. Chem.*, **3**, 1772 (1964); c) T. Shimanouchi and I. Nakagawa, *Spectrochim. Acta*, **18**, 89 (1966); e) T. Shimanouchi and I. Nakagawa, *Inorg. Chem.*, **3**, 1805 (1964).

7) M. Iwata and Y. Saito, *Acta Crystallogr., Sect. B*, **29**, 822 (1973).